



Cite this: *Phys. Chem. Chem. Phys.*,
2022, 24, 22122

On-surface synthesis of ethers through dehydrative coupling of hydroxymethyl substituents†

Yuyi Yan, Fengru Zheng, Zhiwen Zhu, Jiayi Lu, Hao Jiang and Qiang Sun *

On-surface synthesis has been a subject of intensive research during the last decade. Various chemical reactions have been developed on surfaces to prepare compounds and carbon nanostructures, most of which are centered on the carbon–carbon bond formation. Despite the vast progress so far, the diversity of functional groups in organic chemistry has been far less explored in on-surface synthesis. Herein, we study the surface-assisted synthesis of ethers through the homocoupling of hydroxymethyl substituents on Ag(111). By using two hydroxymethyl substituent functionalized molecular precursors with different symmetries, we have achieved the formation of ether chains and rings. High-resolution scanning tunneling microscopy complemented with density functional theory calculations are used to support our findings and offer mechanistic insights into the reaction. This work expands the toolbox of on-surface reactions for the bottom-up fabrication of more sophisticated functional nanostructures.

Received 6th July 2022,
Accepted 30th August 2022

DOI: 10.1039/d2cp03073j

rsc.li/pccp

Introduction

One of the contemporary challenges in the field of nanotechnology lies in the bottom-up construction of molecular architectures with atomic precision. In nature, the ability of molecules to selectively interact with others lays a solid foundation for self-assembly and self-organization processes. The same principle can be applied to the bottom-up construction of molecular nanostructures on surfaces, which has been widely investigated for the last two decades and a variety of supramolecular nanostructures have been fabricated on various surfaces *via* choices of different molecular building blocks.¹ Later on, more studies aimed at covalently bonded nanostructures, which promise more robust intermolecular interactions and more efficient charge transport for practical applications in molecular nanoelectronics and spintronics.^{2–4} In this regard, on-surface synthesis has proven to be a powerful tool, offering two primary advantages: (1) the employment of ultrahigh vacuum (UHV) conditions and catalytic metal surfaces provide a fertile playground for synthesizing unstable products^{5–7} that are hard to obtain with traditional solution-based chemistry; (2) reaction intermediates and products can be accessed in unprecedented detail *via* surface sensitive

techniques, thus providing key mechanistic information on the reaction pathway.^{8–11}

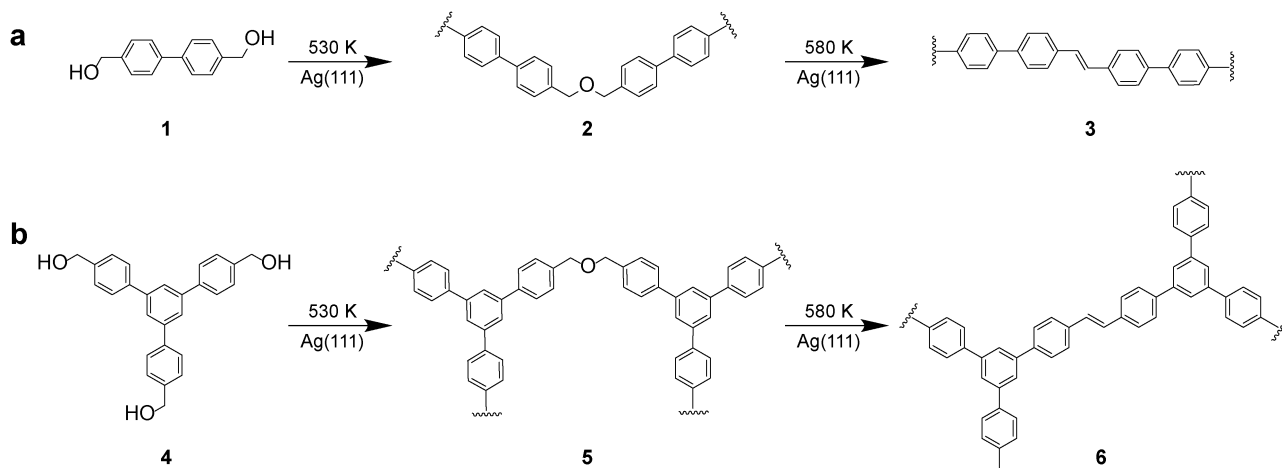
Several important chemical reactions have been developed for preparing new compounds and covalently interlinked nanostructures, such as Ullman coupling,^{12–14} imine formation,^{15,16} dehydration of boronic acids,¹⁷ Bergman cyclization,^{18,19} Glaser coupling,^{20,21} and click reaction,²² to mention a few. Most notably, the formation of intermolecular C–C bonds after activation of the C–X (X = Br, I, or H) bonds has been most extensively studied to fabricate a spectrum of carbon nanostructures. Despite the great progress in on-surface synthesis, the diversity of reaction products is still limited as compared to traditional solution chemistry due to the limited types of on-surface reactions.

Ethers represent a class of organic compounds that contain a group with an oxygen atom connected to two alkyl or aryl groups, which features the C–O–C structure.^{23–25} Despite its importance and ubiquity in nature, the synthesis of ethers in on-surface synthesis is poorly explored to the best of our knowledge. On-surface reaction of molecular precursors with hydroxyl substituents as reactive functional groups should be a promising approach. In this respect, previous work has shown the cleavage of the OH substituent of phenol derivatives and selective C–H activations on surfaces.^{17,26–29} More recently, the formation of intramolecular C–O–C groups by activation of phenol substituents was also demonstrated.^{30,31} The functional groups involved in these works are all bonded to the sp^2 hybridized aryl groups. In contrast to sp^2 -hybridization, sp^3 -hybridization may show different reactivity or result in reaction products of distinct properties.^{32–35}

Materials Genome Institute, Shanghai University, 200444 Shanghai, China.

E-mail: qiangsun@shu.edu.cn

† Electronic supplementary information (ESI) available. See DOI: <https://doi.org/10.1039/d2cp03073j>

Scheme 1 Chemical schemes of the on-surface homocouplings of (a) **1** and (b) **4**.

Herein, we have designed two molecular precursors functionalized with a hydroxymethyl group, which has a methylene bridge ($-\text{CH}_2-$ unit) connected to a hydroxyl group ($-\text{OH}$). The chemical structures of the two precursors, the linear molecule **1** (*4,4'*-bis(hydroxymethyl)biphenyl) and the three-fold symmetric molecule **4** ($[1,1',3,1'',3'',1''']$ -quaterphenyl]-3,3'''-dimethyl alcohol), are displayed in Scheme 1. By high-resolution scanning tunneling microscopy (STM) imaging and manipulations under ultrahigh vacuum (UHV) conditions combined with density functional theory (DFT) calculations, we have succeeded in the fabrication of organic chains and porous ring structures with periodic ether groups through surface assisted dehydrative coupling of the hydroxymethyl group. The reaction is further rationalized by searching for the reaction pathway using DFT-based nudged elastic band (NEB) method calculations.

Results and discussion

Molecule **1** forms ordered network nanostructures after being evaporated on the Ag(111) surface at room temperature (RT, 300 K) (Fig. 1(a) and Fig. S1, ESI[†]). The network structure is reminiscent of the Kagome lattice with additional nodes in the unit cell (see lattice structures in Fig. S1, ESI[†]).³⁶ We can identify the individual molecules from the close-up STM image shown in Fig. 1(b), which appears as a bump. Notably, all of the molecules in the network are connected through a uniform structural motif with both of their hydroxymethyl termini interacting with two molecules. The long-range organization and the uniform structural motif point to intermolecular supramolecular interactions,^{37–39} which arise from the hydroxymethyl substituents. To further identify its atomic-scale structure, we resort to DFT calculations to model the self-assembled nanostructures in the gas phase. The structural motif can be reproduced by three **1** molecules with their hydroxyl groups forming cyclic hydrogen bonding, as indicated in Fig. 1(d). We further map the charge density difference of this motif, where hydrogen bonding interactions are unambiguously displayed. This elementary structural motif underpins both of

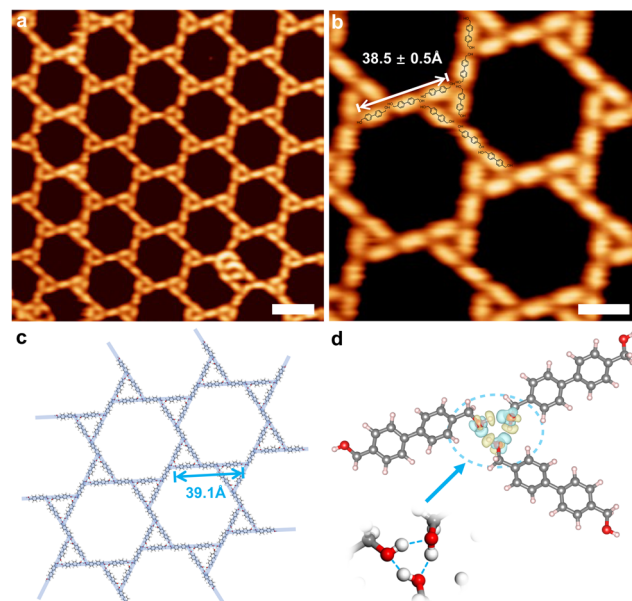


Fig. 1 Self-assembled nanostructure of molecule **1** on Ag(111). (a) Large-scale and (b) close-up STM images showing the formation of a Kagome-like network after deposition of **1** on Ag(111) held at RT. (c) The corresponding DFT-optimized structural model. To better distinguish the Kagome-like arrangement, semitransparent lines are overlaid on the molecular structures. (d) Charge density difference map showing the hydrogen bonding of the three hydroxymethyl substituents, where cyan and yellow isosurfaces indicate charge accumulation and depletion, respectively. Isosurface value at $0.002 \text{ e Bohr}^{-3}$. The structural model without isosurfaces is also displayed with the dashed lines revealing the directionality of the hydrogen bonds. Tunnelling parameters: (a) and (b) $V_t = -1.2 \text{ V}$, $I_t = 20 \text{ pA}$. Scale bars: (a) 4 nm, (b) 2 nm.

the self-assembled nanostructures formed by **1** and **4** (*vide infra*).

Built on the structural motif, the experimentally observed network could be satisfactorily reproduced by the DFT model in Fig. 1(c). We find a perfect agreement between the experimental image and theoretical model; for instance, the line-scan profile

across three molecules along the white arrow in Fig. 1(b) is 38.5 ± 0.5 Å, while the theoretical value is 39.1 Å. Notably, despite the predominant number of pristine **1** molecules on the surface, a careful inspection of the data reveals a very small number (<1%) of molecules being already coupled, which implies a low potential energy barrier of the coupling reaction. The reaction pathway will be discussed by our DFT calculations in the following context.

After annealing the sample at 470 K for 30 minutes, we find an apparent drop in the molecular coverage (roughly 50% of molecules desorb from the surface) and formations of dimerized and trimerized molecules on the surface, as displayed in Fig. 2(a) and (b). The covalent nature of the dimer and trimer is confirmed by moving the trimer structure as a whole with lateral STM manipulations (Fig. S2, ESI†). The dimer and trimer structures can be assigned to the C–O–C coupled ethers by comparisons of the shape and length between the DFT optimized models and the corresponding experimental images (Fig. 2(b) and (g)). Because of the sp^3 hybridized nature of the carbons within the C–O–C ether bonds, two different types of trimers appeared with zigzag and C shapes (see STM images and models in Fig. S3, ESI†), and the ratio between the two trimer structures is about 6:1. We do not find any cyclic structures or longer chains in this phase.

Upon further increasing the temperature to 530 K for 30 minutes, most of the hydroxyl groups are activated, leading to the formation of zigzag-shaped nanowires (Fig. 2(c) and (d)). Remarkably, some nanowires could extend over tens of nanometers (Fig. S4, ESI†). A detailed comparison of the morphology and unit length between the zigzag nanowire with the DFT-relaxed model of the C–O–C coupled ether chain (Fig. 2(d) and (g)) allows us to confirm its formation. Other conceivable structures including the C–O–O–C coupled and C–C coupled molecular chains are also considered. However, agreement is only found for the C–O–C junction (Fig. 2(g) and Fig. S6, ESI†). We also note that the C–O–C group results in an angle of around 107° between the biphenyl units (Fig. 2(d) and (g)). This observation is consistent with the compounds with ether groups in solid and gas phases.⁴⁰ The formation of the ether chains from the coupling of hydroxymethyl groups suggests a dehydration process, which is common for hydroxyl groups in solution chemistry.^{41–43} Note that we do not find any Ag atom incorporated organometallic intermediates as in the coupling of carboxylic substituents on metal surfaces.

The zigzag ether chains could be transformed to straight wires of only a few nanometers after further annealing the sample to 580 K for 30 minutes. These molecular wires are assigned to the carbon–carbon coupled molecular chain, since the carbon–carbon bonds may result in the linear configuration, which cannot be constructed by involving oxygen atoms. Moreover, the unit length of the DFT-relaxed molecular model also coincides with the molecular oligomer (Fig. 2(f) and (h)). More examples of product **3** can be found in Fig. S5 (ESI†). Although it is difficult to distinguish between the C–C single bond and C=C double bond in this nanostructure, we suggest that the carbon–carbon linkage is more likely to be the C=C

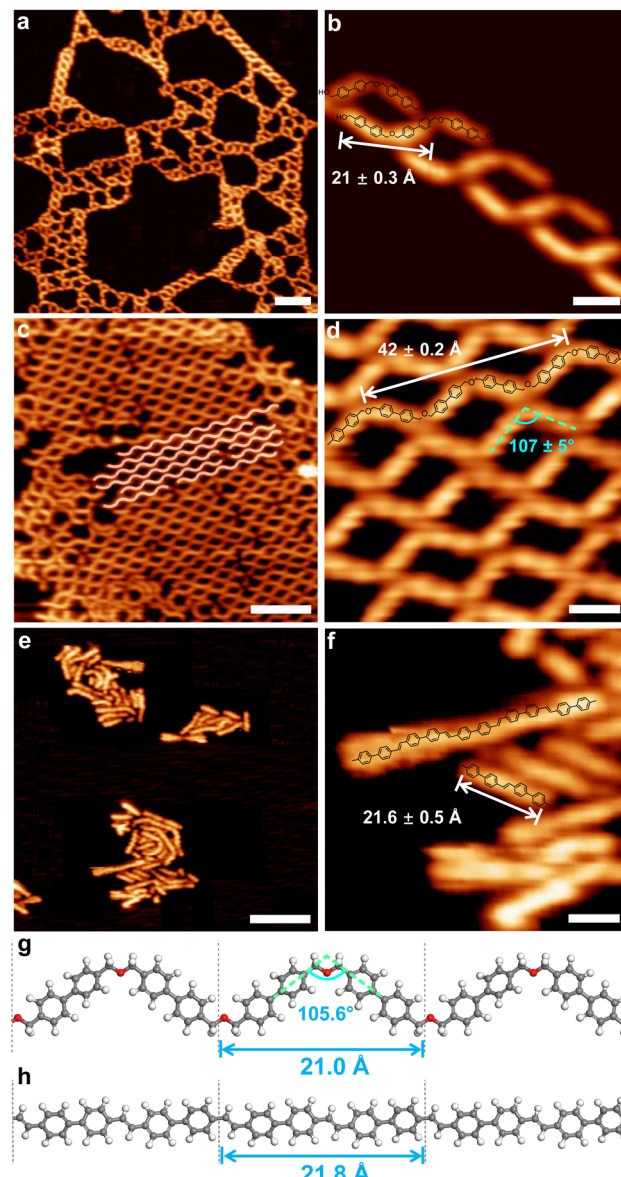


Fig. 2 On-surface reaction of **1**. (a) Large-scale and (b) zoomed-in STM images showing the formation of the C–O–C coupled dimers and trimers after annealing the sample at 470 K for 30 minutes. (c) Large-scale and (d) high-resolution STM images of the C–O–C coupled oligomers after annealing at 530 K for 30 minutes. Wavy lines are overlaid on a few oligomers to illustrate the length of the formed ethers in (c). (e) Large-scale and (f) close-up STM images showing the carbon–carbon coupling chains after further annealing the sample at 580 K for 30 minutes. Corresponding DFT optimized models and the unit lengths of (g) the C–O–C coupled and (h) carbon–carbon coupling chains. A couple of equally scaled chemical structures of the relevant molecules are overlapped in (b), (d) and (f). Tunnelling parameters: (a) and (b) $V_t = -1.0$ V, $I_t = 100$ pA; (c) $V_t = -1.2$ V, $I_t = 50$ pA; (d) $V_t = -0.9$ V, $I_t = 50$ pA; (e) and (f) $V_t = -1.2$ V, $I_t = 100$ pA. Scale bars: (a), (c), (e), 6 nm, (b), (d) and (f), 1 nm.

motif rather than the C–C structure as recent works demonstrated the transformation of alkanyl C–C junctions to alkenyl C=C junctions at high temperatures on metal surfaces.^{44,45}

In order to demonstrate the generality of the dehydrative coupling of hydroxymethyl substituents, complementary to the

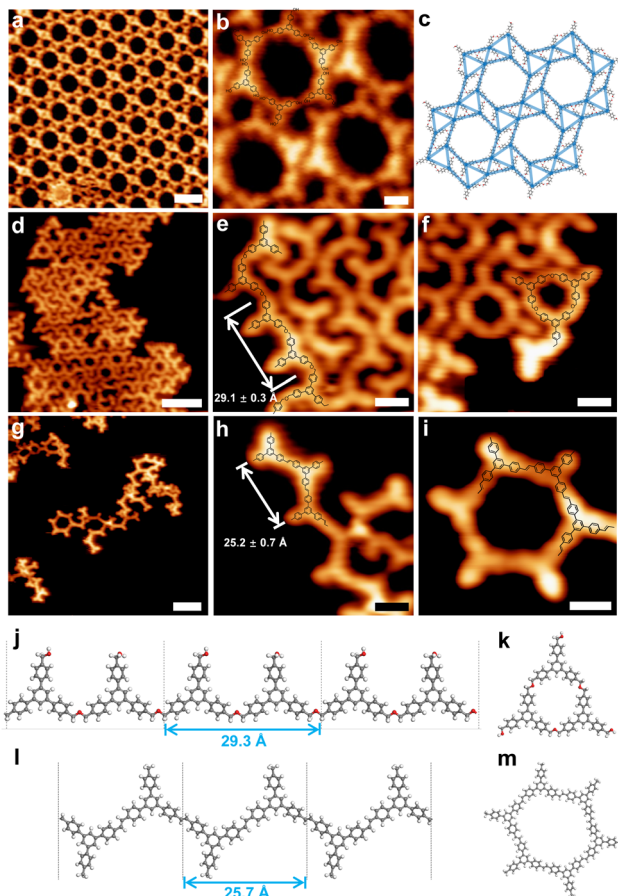


Fig. 3 Self-assembled nanostructure and on-surface reaction of **4** on Ag(111). (a) Large-scale and (b) close-up STM images showing the formation of a porous nanostructure after deposition of **4** on Ag(111) held at RT. (c) The corresponding DFT-optimized structural model and semitransparent lines indicate a hexagonal porous pattern. (d) STM image of the sample prepared at an annealing temperature of 530 K for 30 minutes, leading to the C–O–C coupled products. Zoomed-in STM images disclose the (e) chain and (f) ring structures. (g) STM image of the sample prepared at 580 K, leading to the carbon–carbon coupled products. Zoomed-in STM images disclose the (h) chain and (i) ring structures. (j) and (k) DFT optimized models of the C–O–C coupled chain and ring structures. (l) and (m) DFT optimized models of the carbon–carbon coupled chain and ring structures. The unit lengths in the computed C–O–C and carbon–carbon chains are shown in (j) and (l). Tunneling parameters: (a) and (b) $V_t = -1.5$ V, $I_t = 50$ pA; (d) and (e), (f) $V_t = -0.5$ V, $I_t = 100$ pA, (g) and (h), (i) $V_t = -1.6$ V, $I_t = 50$ pA. Scale bars: (a), (d) and (g), 2 nm, (b), (e), (f), (h) and (i), 1 nm.

linear ditopic **1**, we have designed a three-fold symmetric molecule **4** substituted with three hydroxymethyl groups. The deposition of **4** on Ag(111) kept at RT leads predominantly to a porous pattern which could extend over 50 nm (Fig. 3(a) and Fig. S7, ESI[†]). The corresponding DFT-optimized model is indicated in Fig. 3(c) and Fig. S7b (ESI[†]). The porous network displays an interesting two-dimensional topology after being present by nodes and edges, as shown in Fig. 3(a). Each molecule interacts with six molecules through the elementary hydrogen bonding structural motif indicated in Fig. 1(d). Such a molecular packing fulfills the requirement that all the

hydroxymethyl substituents are in their most stable state, *i.e.*, the cyclic hydrogen bonding motif.

After being prepared at 530 K, we find different structures other than the porous network on the sample. As displayed in the large-scale image in Fig. 3(d) and the high-resolution ones in Fig. 3(e) and (f), the activation of two hydroxymethyl substituents of **4** yields a linear and a ring structure. The length of two repeating units of the linear molecule is measured to be 29.1 ± 0.3 Å (Fig. 3(e)), which fits very well with the calculated result (29.3 Å) from the DFT-optimized model of a C–O–C coupled molecular chain (Fig. 3(j)), thus supporting the formation of ethers through the coupling of hydroxymethyl substituents. DFT-optimized geometries with other plausible junctions are also compared with the experimental data, and agreement is only found for the C–O–C junction (Fig. S10, ESI[†]). The same conclusion is also applied to the ring structure (Fig. 3(f) and (i)). Note that we have not observed extended 2D ether structures, and the ratio of precursor **4** forming circle products and linear products is about 1:3. To verify the covalent bonding of the formed nanostructures, we have tested their robustness by performing lateral STM manipulations on both the chain structure and ring structure (Fig. S8 and S9, ESI[†]). In both cases, the nanostructures are laterally moved without being broken.

By further increasing the annealing temperature to 580 K, there is a further drop in the molecular coverage and we observed carbon–carbon coupled nanostructures (Fig. 3(g)). Both chain structure and ring structure are found as indicated in the close-up images of Fig. 3(h) and (i). However, in this step, only 5% of the precursor **4** form the ring structure. The corresponding DFT-optimized geometries with C–O–C linkages (Fig. 3(l) and (m)) are also consistent with the experimental results. Therefore, as expected, the reaction behaviors of **4** are consistent with **1**, which further supports the dehydrative coupling of hydroxymethyl groups on Ag(111).

To further validate the surface-assisted dehydration of molecule **1** on Ag(111), we have carried out the climbing image nudged elastic band (CI-NEB) method to elucidate the possible reaction mechanism. We used phenylmethanol molecules to simplify the simulation while still capturing key features of the reaction. The computed results of a reaction pathway are summarized in Fig. 4. The reaction begins with a dimer structure with two phenylmethanol molecules stabilized by the H··OH hydrogen bonding in the initial state (IS). From the IS to intermediate state Int1, one OH group detached from one of the molecules captures the hydrogen from the hydroxyl group of the second molecule, which results in a water molecule. The water molecule is stabilized *via* an H··OH hydrogen bond with the O atom of the second molecule. Meanwhile, the two molecules are bonded to the underlying surface atoms. The energy barrier from the IS to Int1 is determined to be 1.12 eV. The progress from Int1 to Int2 reveals the detachment of the water molecule from the molecular complex, which requires 0.42 eV. This energy scale corresponds to a relatively strong hydrogen bond strength.⁴⁶ Finally, the reaction pathway is accomplished by forming the C–O–C bonded dimer structure

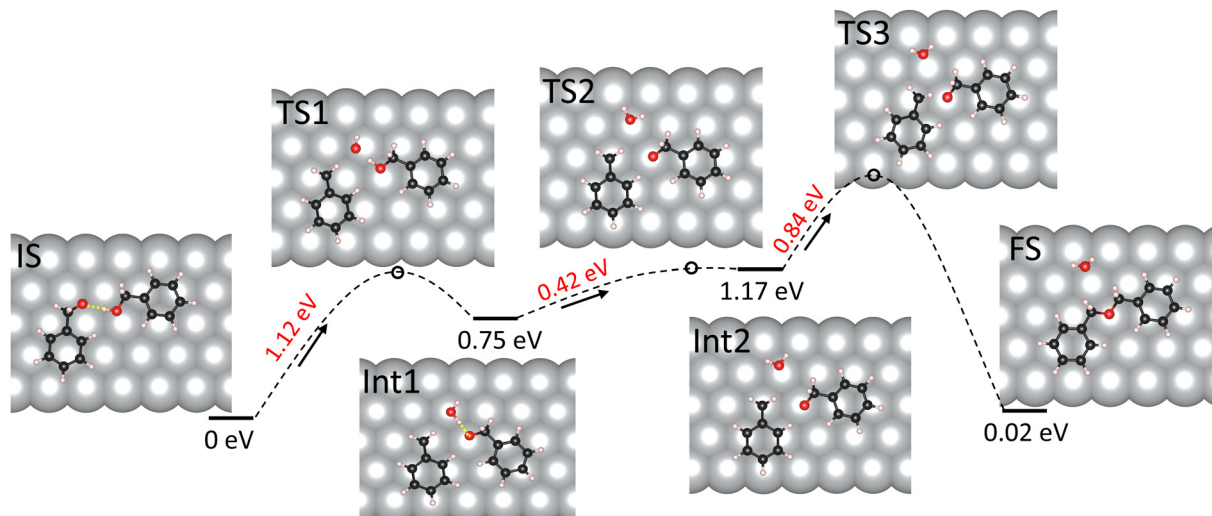


Fig. 4 Theoretical investigation on the reaction pathway. The energy profile of the dehydrative coupling of two phenylmethanol molecules on Ag(111). The computed structures of the initial (IS), transition (TS), intermediate (Int), and final (FS) states are given along the pathway. The relative energies of Int1, Int2 and FS are given with respect to the total energy of the IS. The reaction barriers are given in red. The H···OH hydrogen bondings present in IS and Int1 are marked by yellow dashed lines. Note that the H atom of the hydroxyl groups from the left molecule in the model of SI is beneath the O atom.

from Int2 to the final state (FS). This final elementary step is analogous to the C–C bond formation of molecules with carbon radicals on metal surfaces, proceeding through the breaking of the molecule–substrate bonds to the formation of a new bond.⁴⁷

Thermodynamically, the whole reaction is limited by the first step with the highest energy barrier of 1.12 eV, which agrees with our findings that we start to observe the C–O–C bonded molecule at relatively low temperatures. Although the current reaction pathway shows a negligible energy difference between IS and FS, we note that the water molecule will desorb from the surface to the UHV chamber like other gas molecules,⁴⁸ which results in an irreversible reaction path and facilitates the on-surface dehydrative reaction. Moreover, we have not taken into account the entropic contribution from the desorption of the water molecules, which may also lower the total energy of the FS.

Conclusions

In summary, we have demonstrated the on-surface formation of ethers through the dehydrative coupling of hydroxymethyl substituents. A linear di-topic molecule and a three-fold symmetric tri-topic molecule were designed and studied. Both of the molecules form C–O–C linkages after thermal treatments and yield ethers of chain and ring shapes on the surface, respectively. The reaction products were characterized by a combination of high-resolution UHV-STM imaging and DFT calculations. The reaction pathways were further rationalized by DFT-based NEB calculations, which helps to identify the key reaction intermediates and provide mechanisms for the on-surface reaction. These findings expanded the on-surface reactions toolbox for the bottom-up fabrication of organic nanomaterials, and it provides a feasible strategy to generate

a new family of organic chains and networks with ether linkages on surfaces. We expect the realization of more sophisticated carbon nanostructures with heteroatoms.

Conflicts of interest

The authors declare no competing financial interest.

Acknowledgements

This work was supported by the National Natural Science Foundation of China (No. 22072086). We thank Jiong Yang and Mingjia Yao at Shanghai University for help in setting up the CI-NEB calculations.

References

- 1 L. Bartels, Tailoring molecular layers at metal surfaces, *Nat. Chem.*, 2010, 2(2), 87.
- 2 K. Leng, I. Abdelwahab, I. Verzhbitskiy, M. Telychko, L. Chu, W. Fu, X. Chi, N. Guo, Z. Chen and Z. Chen, *et al.*, Molecularly thin two-dimensional hybrid perovskites with tunable optoelectronic properties due to reversible surface relaxation, *Nat. Mater.*, 2018, 17(10), 908.
- 3 W. R. Browne and B. L. Feringa, Making molecular machines work, *Nat. Nanotechnol.*, 2006, 1(1), 25.
- 4 V. Balzani, A. Credi, F. M. Raymo and J. F. Stoddart, Artificial molecular machines, *Angew. Chem., Int. Ed.*, 2000, 39(19), 3348.
- 5 L. Grill and S. Hecht, Covalent on-surface polymerization, *Nat. Chem.*, 2020, 12(2), 115.

- 6 S. Clair and D. G. de Oteyza, Controlling a chemical coupling reaction on a surface: Tools and strategies for on-surface synthesis, *Chem. Rev.*, 2019, **119**(7), 4717.
- 7 Q. Shen, H.-Y. Gao and H. Fuchs, Frontiers of on-surface synthesis: From principles to applications, *Nano Today*, 2017, **13**, 77.
- 8 S.-W. Hla, L. Bartels, G. Meyer and K.-H. Rieder, Inducing all steps of a chemical reaction with the scanning tunneling microscope tip: Towards single molecule engineering, *Phys. Rev. Lett.*, 2000, **85**(13), 2777.
- 9 N. Pavliček, B. Schuler, S. Collazos, N. Moll, D. Pérez, E. Guitián, G. Meyer, D. Peña and L. Gross, On-surface generation and imaging of arynes by atomic force microscopy, *Nat. Chem.*, 2015, **7**(8), 623.
- 10 G. de Oteyza Dimas, P. Gorman, Y.-C. Chen, S. Wickenburg, A. Riss, J. Mowbray Duncan, G. Etkin, Z. Pedramrazi, H.-Z. Tsai and A. Rubio, *et al.*, Direct imaging of covalent bond structure in single-molecule chemical reactions, *Science*, 2013, **340**(6139), 1434.
- 11 B. Schuler, S. Fatayer, F. Mohn, N. Moll, N. Pavliček, G. Meyer, D. Peña and L. Gross, Reversible Bergman cyclization by atomic manipulation, *Nat. Chem.*, 2016, **8**(3), 220.
- 12 W. Wang, X. Shi, S. Wang, M. A. Van Hove and N. Lin, Single-molecule resolution of an organometallic intermediate in a surface-supported Ullmann coupling reaction, *J. Am. Chem. Soc.*, 2011, **133**(34), 13264.
- 13 J. Cai, P. Ruffieux, R. Jaafar, M. Bieri, T. Braun, S. Blankenburg, M. Muoth, A. P. Seitsonen, M. Saleh and X. Feng, *et al.*, Atomically precise bottom-up fabrication of graphene nanoribbons, *Nature*, 2010, **466**(7305), 470.
- 14 M. Bieri, M.-T. Nguyen, O. Gröning, J. Cai, M. Treier, K. Aït-Mansour, P. Ruffieux, C. A. Pignedoli, D. Passerone and M. Kastler, *et al.*, Two-dimensional polymer formation on surfaces: Insight into the roles of precursor mobility and reactivity, *J. Am. Chem. Soc.*, 2010, **132**(46), 16669.
- 15 S. Weigelt, C. Busse, C. Bombis, M. M. Knudsen, K. V. Gothelf, T. Strunskus, C. Wöll, M. Dahlbom, B. Hammer and E. Lægsgaard, *et al.*, Covalent interlinking of an aldehyde and an amine on a Au(111) surface in ultrahigh vacuum, *Angew. Chem., Int. Ed.*, 2007, **46**(48), 9227.
- 16 X.-H. Liu, C.-Z. Guan, S.-Y. Ding, W. Wang, H.-J. Yan, D. Wang and L.-J. Wan, On-surface synthesis of single-layered two-dimensional covalent organic frameworks *via* solid-vapor interface reactions, *J. Am. Chem. Soc.*, 2013, **135**(28), 10470.
- 17 N. A. A. Zwaneveld, R. Pawlak, M. Abel, D. Catalin, D. Gimès, D. Bertin and L. Porte, Organized formation of 2D extended covalent organic frameworks at surfaces, *J. Am. Chem. Soc.*, 2008, **130**(21), 6678.
- 18 Q. Sun, C. Zhang, Z. Li, H. Kong, Q. Tan, A. Hu and W. Xu, On-Surface formation of one-dimensional polyphenylene through Bergman cyclization, *J. Am. Chem. Soc.*, 2013, **135**(23), 8448.
- 19 A. Riss, S. Wickenburg, P. Gorman, L. Z. Tan, H.-Z. Tsai, D. G. de Oteyza, Y.-C. Chen, A. J. Bradley, M. M. Ugeda and G. Etkin, *et al.*, Local electronic and chemical structure of oligo-acetylene derivatives formed through radical cyclizations at a surface, *Nano Lett.*, 2014, **14**(5), 2251.
- 20 H.-Y. Gao, H. Wagner, D. Zhong, J.-H. Franke, A. Studer and H. Fuchs, Glaser coupling at metal surfaces, *Angew. Chem., Int. Ed.*, 2013, **52**(14), 4024.
- 21 Y.-Q. Zhang, N. Kepcija, M. Kleinschrodt, K. Diller, S. Fischer, A. C. Papageorgiou, F. Allegretti, J. Björk, S. Klyatskaya and F. Klappenberger, *et al.*, Homo-coupling of terminal alkynes on a noble metal surface, *Nat. Commun.*, 2012, **3**(1), 1286.
- 22 F. Bebensee, C. Bombis, S.-R. Vadapoo, J. R. Cramer, F. Besenbacher, K. V. Gothelf and T. R. Linderoth, On-surface azide–alkyne cycloaddition on Cu(111): Does it “click” in ultrahigh vacuum?, *J. Am. Chem. Soc.*, 2013, **135**(6), 2136.
- 23 H. Feuer and J. Hooz, Methods of formation of the ether linkage. *The Ether Linkage*, 1967, vol. 1967, p. 445.
- 24 D. J. Blundell and B. N. Osborn, The morphology of poly(aryl-ether-ether-ketone), *Polymer*, 1983, **24**(8), 953.
- 25 K. L. Jensen, G. Dickmeiss, H. Jiang, L. Albrecht and K. A. Jørgensen, The diarylprolinol silyl ether system: A general organocatalyst, *Acc. Chem. Res.*, 2012, **45**(2), 248.
- 26 A. C. Marele, R. Mas-Ballesté, L. Terracciano, J. Rodríguez-Fernández, I. Berlanga, S. S. Alexandre, R. Otero, J. M. Gallego, F. Zamora and J. M. Gómez-Rodríguez, Formation of a surface covalent organic framework based on polyester condensation, *Chem. Commun.*, 2012, **48**(54), 6779.
- 27 F. Bebensee, K. Svane, C. Bombis, F. Masini, S. Klyatskaya, F. Besenbacher, M. Ruben, B. Hammer and T. Linderoth, Adsorption and dehydrogenation of tetrahydroxybenzene on Cu(111), *Chem. Commun.*, 2013, **49**(81), 9308.
- 28 F. De Marchi, G. Galeotti, M. Simenas, E. E. Tornau, A. Pezzella, J. MacLeod, M. Ebrahimi and F. Rosei, Room-temperature surface-assisted reactivity of a melanin precursor: Silver metal–organic coordination versus covalent dimerization on gold, *Nanoscale*, 2018, **10**(35), 16721.
- 29 F. Bebensee, K. Svane, C. Bombis, F. Masini, S. Klyatskaya, F. Besenbacher, M. Ruben, B. Hammer and T. R. Linderoth, A surface coordination network based on copper adatom trimers, *Angew. Chem., Int. Ed.*, 2014, **53**(47), 12955.
- 30 H. Kong, S. Yang, H. Gao, A. Timmer, J. P. Hill, O. Diaz Arado, H. Möning, X. Huang, Q. Tang and Q. Ji, *et al.*, Substrate-mediated C–C and C–H coupling after dehalogenation, *J. Am. Chem. Soc.*, 2017, **139**(10), 3669.
- 31 Q. Li, B. Yang, H. Lin, N. Aghdassi, K. Miao, J. Zhang, H. Zhang, Y. Li, S. Duhm and J. Fan, *et al.*, Surface-controlled mono/diselective ortho C–H bond activation, *J. Am. Chem. Soc.*, 2016, **138**(8), 2809.
- 32 X. Yu, L. Cai, M. Bao, Q. Sun, H. Ma, C. Yuan and W. Xu, On-surface synthesis of graphyne nanowires through stepwise reactions, *Chem. Commun.*, 2020, **56**(11), 1685.
- 33 Q. Sun, L. Cai, Y. Ding, H. Ma, C. Yuan and W. Xu, Single-molecule insight into Wurtz reactions on metal surfaces, *Phys. Chem. Chem. Phys.*, 2016, **18**(4), 2730.
- 34 Q. Sun, X. Yu, M. Bao, M. Liu, J. Pan, Z. Zha, L. Cai, H. Ma, C. Yuan and X. Qiu, *et al.*, Direct formation of C–C triple-bonded structural motifs by on-surface dehalogenative homocouplings of tribromomethyl-substituted arenes, *Angew. Chem., Int. Ed.*, 2018, **57**(15), 4035.

- 35 Q. Sun, R. Zhang, J. Qiu, R. Liu and W. Xu, On-surface synthesis of carbon nanostructures, *Adv. Mater.*, 2018, **30**(17), 1705630.
- 36 X. Li, D. Han, T. Qin, J. Xiong, J. Huang, T. Wang, H. Ding, J. Hu, Q. Xu and J. Zhu, Selective synthesis of Kagome nanoporous graphene on Ag(111) *via* an organometallic template, *Nanoscale*, 2022, **14**(16), 6239.
- 37 X. Peng, Y. Geng, M. Zhang, F. Cheng, L. Cheng, K. Deng and Q. Zeng, Guest selectivity in the supramolecular host networks fabricated by van der Waals force and hydrogen bond, *Nano Res.*, 2019, **12**(3), 537.
- 38 R. Adhikari, J. Kuliga, M. Ruppel, N. Jux, H. Marbach and H.-P. Steinrück, Self-assembled 2D-coordination kagome, quadratic, and close-packed hexagonal lattices formed from a cyano-functionalized benzoporphyrin on Cu(111), *J. Phys. Chem. C*, 2021, **125**(13), 7204.
- 39 T. Yokoyama, S. Yokoyama, T. Kamikado, Y. Okuno and S. Mashiko, Selective assembly on a surface of supramolecular aggregates with controlled size and shape, *Nature*, 2001, **413**(6856), 619.
- 40 K. Vojinovic, U. Losehand and N. W. Mitzel, Dichlorosilane-dimethyl ether aggregation: A new motif in halosilane adduct formation, *Dalton Trans.*, 2004, 2578, DOI: [10.1039/B405684A10.1039/B405684A\(16\)](#).
- 41 R. Mueller, J. Yang, C. Duan, E. Pop, L. H. Zhang, T.-B. Huang, A. Denisenko, O. V. Denisko, D. C. Oniciu and C. L. Bisgaier, *et al.*, Long hydrocarbon chain ether diols and ether diacids that favorably alter lipid disorders *in vivo*, *J. Med. Chem.*, 2004, **47**(21), 5183.
- 42 K. Arai and T. Shikata, Hydration/dehydration behavior of cellulose ethers in aqueous solution, *Macromolecules*, 2017, **50**(15), 5920.
- 43 T. Shikata, M. Okuzono and N. Sugimoto, Temperature-dependent hydration/dehydration behavior of poly(ethylene oxide)s in aqueous solution, *Macromolecules*, 2013, **46**(5), 1956.
- 44 A. Kinikar, M. Di Giovannantonio, J. I. Urgel, K. Eimre, Z. Qiu, Y. Gu, E. Jin, A. Narita, X.-Y. Wang and K. Müllen, *et al.*, On-surface polyarylene synthesis by cycloaromatization of isopropyl substituents, *Nat. Synth.*, 2022, **1**(4), 289.
- 45 X. Li, K. Niu, J. Zhang, X. Yu, H. Zhang, Y. Wang, Q. Guo, P. Wang, F. Li and Z. Hao, *et al.*, Direct transformation of *n*-alkane into all-trans conjugated polyene via cascade dehydrogenation, *Natl. Sci. Rev.*, 2021, **8**(10), nwab093.
- 46 T. Steiner, The hydrogen bond in the solid state, *Angew. Chem., Int. Ed.*, 2002, **41**(1), 48.
- 47 J. Björk, F. Hanke and S. Stafström, Mechanisms of halogen-based covalent self-assembly on metal surfaces, *J. Am. Chem. Soc.*, 2013, **135**(15), 5768.
- 48 H.-Y. Gao, P. A. Held, M. Knor, C. Mück-Lichtenfeld, J. Neugebauer, A. Studer and H. Fuchs, Decarboxylative polymerization of 2,6-naphthalenedicarboxylic acid at surfaces, *J. Am. Chem. Soc.*, 2014, **136**(27), 9658.